Revisiting the molecular interactions between the tumor protein TCTP and the drugs sertraline/thioridazine.

Florian Malard, Eric Jacquet, Naima Nhiri, Christina Sizun, Amélie Chabrier, Samir Messaoudi, Jérôme Dejeu, Stéphane Betzi, Xu Zhang, Aurélien Thureau, et al.

The manuscript has been accepted and published in the journal ChemMedChem
(http://dx.doi.org/10.1002/cmdc.202100528)

Revisiting the molecular interactions between the tumor protein TCTP and the drugs sertraline/thioridazine.

Florian Malard[a], Eric Jacquet[a], Naima Nhiri[a], Christina Sizun[a], Amélie Chabrier[b], Samir Messaoudi[b], Jérôme Dejeu[c], Stéphane Betzi[d], Xu Zhang[d], Aurélien Thureau[e], and Ewen Lescop*[a]

[a] Florian Malard, FM, PhD
Eric Jacquet, EJ, PhD
Naima Nhiri, NJ, PhD
Christina Sizun, CS, PhD
Ewen Lescop, EL, PhD

Department: Analytical and Structural Chemistry and Biology
Institution: Institut de Chimie des Substances Naturelles, CNRS, Université Paris- Saclay
Address 1: 1 av. de la terrasse, 91198 Gif-sur-Yvette, France
E-mail: ewen.lescop@cnrs.fr

[b] Amélie Chabrier, AC, PhD
Samir Messaoudi, SM, PhD
Université Paris-Saclay, BioCIS, Faculté de Pharmacie, CNRS, 92290, Châtenay-Malabry, France.

[c] Jérôme Dejeu, JD, PhD
Department: Département de Chimie Moléculaire
Institution: Univ. Grenoble Alpes, CNRS
Address 2: 570 rue de la chimie, CS 40700, Grenoble 38000, France

[d] Stéphane Betzi, SB, PhD
Xu Zhang, XZ, PhD

Department:
Institution: Centre de Recherche en Cancérologie de Marseille (CRCM), CNRS, Aix-Marseille Université, Inserm, Institut Paoli-Calmettes
Address 3: 27 bd Lei Roure, 13273 Marseille CEDEX 9, France

[e] Aurélien Thureau, AT, PhD

Department: -
Institution: Synchrotron SOLEIL
Address 4: 91190 Saint-Aubin, France

Supporting information for this article is given via a link at the end of the document.

Abstract: TCTP protein is a pharmacological target in cancer and TCTP inhibitors such as sertraline have been evaluated in clinical trials. The direct interaction of TCTP with the drugs sertraline and thioridazine has been reported in vitro by SPR experiments to be in the ~30-50 µM Kd range (Amson et al. Nature Med 2012), supporting a TCTP-dependent mode of action of the drugs on tumor cells. However, the molecular details of the interaction remain elusive although they are crucial to improve the efforts of on-going medicinal chemistry. In addition, TCTP can be phosphorylated by the Plk-1 kinase, which is indicative of poor prognosis in several cancers. The impact of phosphorylation on TCTP structure/dynamics and binding with therapeutical ligands remains unexplored. Here, we combined NMR, TSA, SPR, BLI and ITC techniques to probe the molecular interactions between TCTP with the drugs sertraline and thioridazine. We reveal that drug binding is much weaker than reported with an apparent ~mM Kd and leads to protein destabilization that obscured the analysis of the published SPR data. We further demonstrate by NMR and SAXS that TCTP S46 phosphorylation does not promote tighter interaction between TCTP and sertraline. Accordingly, we question the supported model in which sertraline and thioridazine directly interact with isolated TCTP in tumor cells and discuss alternative modes of action for the drugs in light of current literature.

Introduction

The Translationally-Controlled Tumor Protein (TCTP) protein, aka HRF (Histamine Release Factor) or fortilin, is a 172 amino acid globular protein well conserved across species[1]. TCTP binds dozens of proteins and acts in several key cellular functions such as immune response, apoptosis, DNA repair, transcription or protein synthesis with impacts on cell-cycle progression, development, growth, proliferation, survival, and malignant transformation[2,3,4,5,6,7]. The pro-survival properties of TCTP are amongst the best-documented functions of the protein and TCTP acts synergistically through distinct pathways to inhibit cell death and to favor cell proliferation. These pathways include the enhancement of the anti-apoptotic properties of the Bcl-2 family proteins Bcl-xL and Mcl-1 at the mitochondria[8,9,10,11], of the stress sensor IRE1α [12] and of

the growth factor-beta stimulated clone-22 (TSC)[13], and include blocking Ca^{2+}-dependent apoptotic pathways[14]. TCTP is also involved in a negative regulatory loop with the major tumor suppressor p53 and overexpression of TCTP leads to reduced p53 levels, which contributes to maintain the malignant phenotypes in cells[15,16,17,18]. TCTP can directly interact with the DNA binding domain of p53 to prevent the transcriptional activation of Bax[16] and can also bind the E3 ligase MDM2 to inhibit its auto-ubiquitinylation, which leads to increased MDM2-mediated p53 degradation[17,19]. In addition, TCTP is also able to protect cells from apoptosis triggered by serum deprivation[20] or upon drug treatment and may thus play a role in drug resistance[8,21,22]. A recent study also highlighted the role of extracellular TCTP in the recruitment of polymorphonuclear myeloid-derived suppressor cells in the tumor microenvironment, thus contributing to tumor growth[23].

The structure of TCTP contains a globular domain formed by three α-helices and eleven β-strands forming a β-tent[1]. One notable feature is the 30 amino acid long flexible insertion loop[24,25] containing one highly conserved TCTP signature and three identified Polo-like kinase 1 (Plk-1) phosphorylation sites (S46, S64 and T65)[1]. TCTP phosphorylation is functionally important during cell division. Indeed, TCTP associates with and stabilizes the mitotic spindle and is dissociated upon Plk-1 mediated phosphorylation at S46 and S64, allowing metaphase completion and termination of both mitosis[26,27] and meiosis[28]. In addition, S46A mutation in TCTP leads to an increase in apoptosis and in multinucleated cells[26]. Phosphorylation of TCTP further modifies the subcellular localization of the protein[26,29,30] and has been proposed to be a biomarker of Plk-1 level and kinase activity, with potential interest in anti-tumor drug design strategy targeting Plk-1[29,31]. The strict conservation of S46, but not of S64 or T65, in higher eukaryotes further reflects the crucial role of S46 in TCTP biology. In vitro, Plk-1 can phosphorylate TCTP at position S46 but not at position S64[32], and T65 phosphorylation has also been reported[29]. Taken together the Plk-1 phosphorylated state of TCTP may be significantly populated in tumor cells but the structural impact of phosphorylation is yet unclear. In our recent modeling study we proposed that phosphorylation may induce a conformational and dynamic change in the loop to control protein-protein interaction[24].

The accumulating knowledge on TCTP has made it an attractive target for therapeutic strategies in cancers [2,3,4,5,6,7,33,34,35]. Indeed its overexpression in many tumor cell types[34] confers tumor cells with increased survival and chemoresistance, and TCTP depletion by silencing approaches or by small molecules render tumor cells more sensitive to apoptosis and treatment, thus reducing oncogenic traits [18,33,34,36,37,38,39,40,41,42,43,44]. The most promising approach to target TCTP in cancer was introduced by the group of A. Telerman and R. Amson[34]. They showed the growth inhibitory effect of anti-histaminic drugs hydroxyzine and promethazine on U937 cells in the 10μM concentration range which was accompanied by reduced TCTP intracellular levels[37]. Other structurally related drugs such as the antipsychotic thioridazine or the antidepressant sertraline had similar effects on cytotoxicity and TCTP levels[37]. Interestingly, TCTP reduction led to p53 level restoration and reactivation, most likely through the TCTP/MDM2/p53 pathway described above[17]. Sertraline went into clinical studies for cancer treatment[34], including an on-going phase I/II clinical trial against refractory acute myeloid leukemia. Sertraline and thioridazine have been shown to directly interact with TCTP and dissociation constants Kd of 47 μM and 34 μM were derived respectively from Surface Plasmon Resonance (SPR)[17], albeit with yet uncharacterized binding mode at the atomic level. In addition, the two drugs were shown also by SPR to disrupt *in vitro* the TCTP/MDM2 interaction, providing a rationale for the p53 level restoration upon drug treatment[17]. How phosphorylation impacts TCTP interaction network, including with drugs targeting TCTP is still elusive. Nevertheless using the SPR technique, S->E mutations mimicking phosphoserine residues at positions 46 and 64 were found to abolish the interaction of TCTP with MDM2 and ligands[17], and pointed to the long internal loop as a binding hotspot and a potential role of phosphorylation in TCTP binding profile. This binding mode is also supported by *in silico* docking studies that revealed a binding site near S46 and S64 in the hinge region of the internal loop for antihistaminic drugs that also induce TCTP cellular reduction[43].

Despite all the efforts to understand TCTP biology and to develop anti-TCTP therapeutic strategies, and despite evidence of interaction by techniques such as SPR or MST[17,43], structural data at the molecular and atomic levels regarding the interaction between TCTP and active compounds such as sertraline or thioridazine are missing, thus hampering the progress of drug development. In this work, we combined highly complementary structural and thermodynamic approaches including Nuclear Magnetic Resonance (NMR) spectroscopy, Small-Angle X-Ray scattering (SAXS), Thermal Shift Assays (TSA), Surface Plasmon Resonance (SPR), Bio-layer interferometry (BLI), and Isothermal Titration Calorimetry (ITC) to validate the molecular interactions and further characterize the complexes between TCTP and the sertraline and thioridazine drugs. Since the phosphorylated state of TCTP might be relevant in tumor cells we extended the structural and binding studies to the Plk-1-derived pS46-TCTP protein. We could demonstrate that interaction of TCTP with sertraline and thioridazine is very weak (in the mM range) and leads to protein destabilization at high compound concentrations without protein specificity. Our results thus invite to reinvestigate the TCTP-dependent and TCTP-independent modes of action of these drugs, and their roles as TCTP inhibitors.

Results

Relevance and control of recombinant TCTP protein.

In this work, we expressed the human TCTP protein in fusion with a N-Terminal polyhistidine tag. The tag was kept for the ITC study but removed for NMR, SPR, BLI and TSA studies. Upon purification and removal of the affinity tag, the final sequence reproduced the UniProtKB fasta reference (UniProt P13693) for the native TCTP protein plus an additional glycine residue at the N-terminus of protein. Note that the TCTP construct used to show the binding of sertraline/thioridazine [17] and of the Mcl-1 and Bcl-xL proteins to TCTP [11] contained

two extra Gly-Pro residues at the N-Terminus. Prior to protein-drugs interaction studies, we ensured that binding properties and folding of our recombinant TCTP were consistent with existing literature. Feng et al. have provided reference NMR fingerprints for a human TCTP protein containing an extra C-terminal polyhistidine tag, and deciphered the binding mode of the protein with calcium ions[25] and with Eukaryotic Elongation Factor 1B[45]. In our recent study[24], we could obtain very similar NMR data as Feng et al. regarding the structure/dynamics and calcium ion binding properties. Preliminary NMR studies in our lab (Fig S1) confirmed the binding of our TCTP protein with human Bcl-xL proteins, in full agreement with Thebault et al. [11]. Altogether, these elements reasonably support the limited impact of extra residues at the N- or C-termini of the protein and the relevance of the TCTP construct we designed for protein-drugs interaction studies.

NMR study of TCTP/drugs interaction.

NMR is a method of choice for drug-screening and binding site mapping. In the NMR spectrum, each NMR signal has unique chemical shift which reports on the local chemical environment of the corresponding nucleus. Accordingly, the presence of a binder in the vicinity of the atoms triggers chemical shift variations, thus allowing to detect the interaction, to delineate the binding hot-spot and to compute binding parameters. We recorded 2D ^{15}N SOFAST-HMQC experiments, allowing to map every H-N bond within TCTP backbone and side-chains. Each NMR cross-peak was assigned previously to one TCTP residue[24,25], except for prolines that do not contain H-N bonds, the extra glycine resulting from TEV cleavage and asparagine R51 that remained invisible in the spectra. Herein, we aimed at using solution-state NMR to confirm the TCTP/drug molecular interactions unveiled by SPR experiments[17] and to map the binding interface by performing NMR titrations of ^{15}N labeled TCTP with sertraline or thioridazine. By contrast with thioridazine, sertraline was poorly soluble in aqueous buffers and gave broad ^{1}H NMR signals. Thus, we first optimized the buffer composition. Adding 2.5% DMSO-d6 increased the solubility of sertraline to at least 500 µM as judged from narrow ^{1}H NMR signals of sertraline. Note that TCTP structure was not significantly perturbed at 2.5% DMSO as judged from ^{15}N HSQC spectra (Figure S2). Next, we performed NMR titration experiments of TCTP with drugs (Figure 1). The reference spectrum and the spectrum after addition of 200 µM sertraline (Figure 1A) or 500 µM thioridazine (Figure 1B) were virtually identical. Under the concentrations of these experiments (100 µM TCTP / 200 µM sertraline), and assuming a Kd dissociation constant of 47 µM for sertraline [17], one would expect the protein to be predominantly (73%) in the bound state and clear NMR spectral changes should occur. A similar analysis could be done for thioridazine with reported 34 µM Kd. The current NMR data then do not support a strong ~30-50 µM binding mode for the two molecules. At sertraline concentration larger than 400 µM, we observed a decrease in intensity of TCTP signals together with slight chemical shift perturbation (Figure 1A). Both observations were consistent with sertraline inducing at high concentration TCTP aggregation and precipitation and a shift in the well-characterized monomer-dimer equilibrium[24], explaining the observed chemical shift perturbation. From the drug side, the addition of sertraline and thioridazine was monitored in the respective 1D 1H spectra (Figures 1C-1D). The NMR signals of sertraline at low (25 µM) concentration was still narrow despite the excess (100 µM) of protein, in disagreement with the potential dramatic change in tumbling properties of the molecule expected upon binding (Figures 1C). For thioridazine, signal intensity of the added drug increased consistently with concentrations but without chemical shift variations (Figure 1D). This, again, was not consistent with strong ~30-50 µM interaction. We consented to more efforts and engaged in Saturation Transfer Difference (STD) NMR, a technique frequently deployed to detect interactions of medium-weak (µM-mM) affinity between protein and drug. Upon saturation of methyl resonances in TCTP protein, no signal could be seen in the STD spectrum of sertraline (Figure 1C). In the limit of kinetic steps not compatible with efficient intermolecular saturation transfer, the absence of positive signals in the STD spectrum of sertraline further indicates the absence of detected interaction with TCTP. Altogether, NMR could not detect any interaction between TCTP and sertraline or thioridazine at drug concentration below 200 – 400 µM, while sertraline tended to destabilize TCTP at higher concentrations.

TCTP-sertraline interaction from ITC techniques

Since our NMR experiments could not reveal interactions in the expected ~50 µM dissociation constant, we also used ITC experiments to probe TCTP/sertraline interaction. Upon sertraline injection, no heat release was observed at 25°C up to 2 molar equivalents (200 µM sertraline) (see Figure 2). In order to evaluate if the interaction would be stuck in an enthalpic trap we also collected data at 35°C and no heat release was observed. Taken together, the ITC measurements could not detect any interaction between TCTP and sertraline under conditions where heat release would be expected for a dissociation constant in the 10-100 µM range, further confirming the previous NMR experiment.

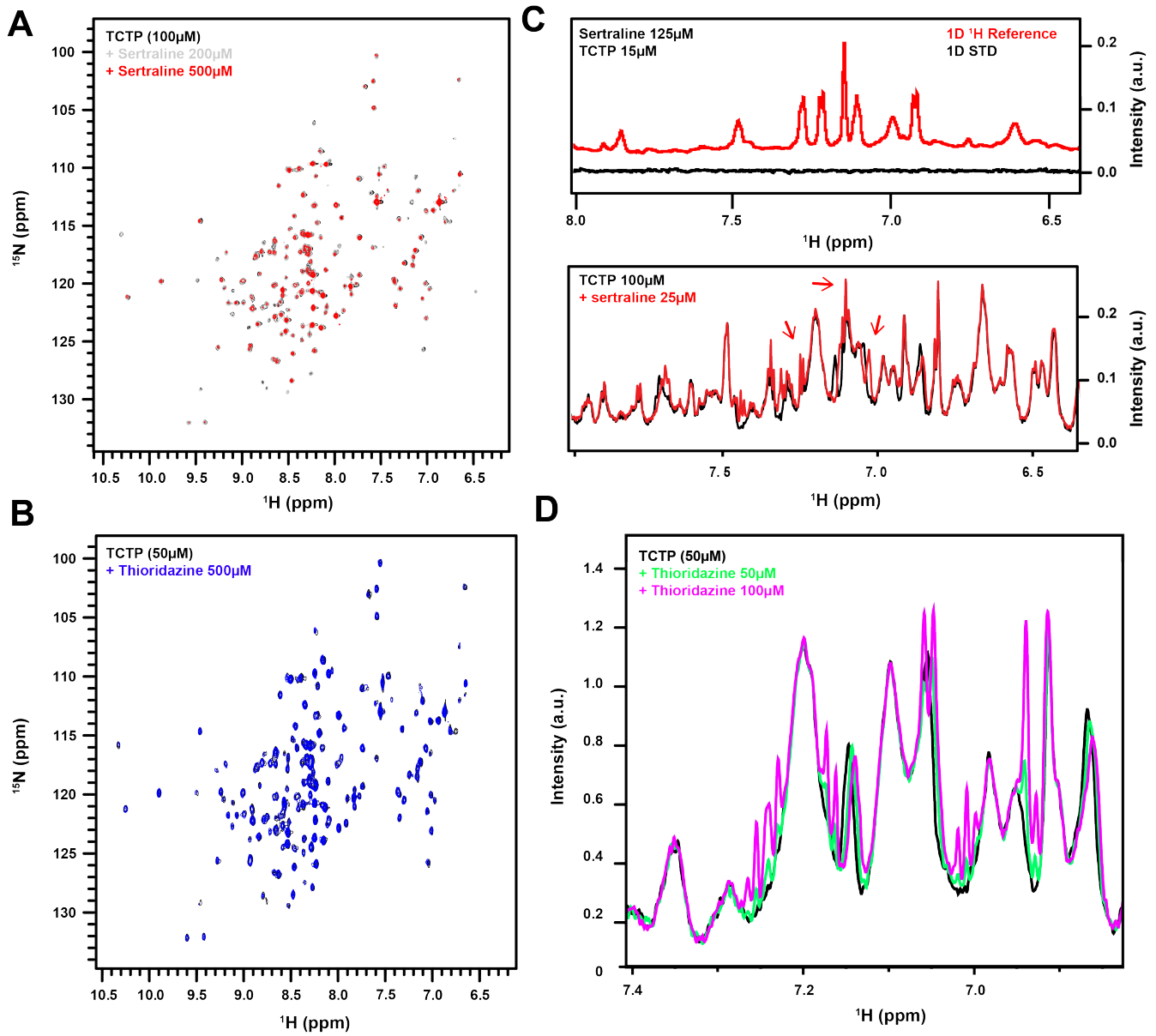

Figure 1. NMR study of TCTP/drug interaction. Comparison of ^{15}N SOFAST-HMQC (panel A) collected before (black) and after addition of 200 μM (grey) and 500 μM sertraline (red) on a sample containing 100 μM ^{15}N labeled TCTP dissolved in 10 mM HEPES pH 7.4, 150 mM NaCl, 2 mM TCEP, 2.5% DMSO-d6, 95% / 5% H_2O / D_2O. The Saturation Transfer Difference (STD) spectra are shown in panel C with the reference (red) and STD (black) experiments. The STD spectrum was calculated as the difference spectrum between the reference and saturated spectra in which the 50-ms Gaussian selective pulse train was applied at -62.5 ppm and 0 ppm respectively. Note that the methyl group of residues I17 and V73 resonate near 0 ppm. The ^{1}H spectra before (black) and after (red) addition of 25μM sertraline is shown in panel C (bottom). The growing crosspeaks labeled with arrows correspond to sertraline signals and are at the chemical shifts expected for sertraline in absence of protein. Panel B shows the ^{15}N SOFAST-HMQC collected before (black) and after (blue) addition of 500 μM thioridazine to a sample containing 50 μM ^{15}N labeled TCTP dissolved in 10 mM HEPES pH 7.4, 150 mM NaCl, 2 mM TCEP, 95% / 5% H_2O / D_2O. Panel D shows the 1D ^{1}H spectra collected at 0 (black), 50 μM (green) and 100 μM (magenta) thioridazine concentrations. The growing crosspeaks correspond to thioridazine signals and are at the chemical shifts expected for thioridazine in absence of protein. All spectra were collected at 25°C and at ^{1}H 800 MHz frequency.

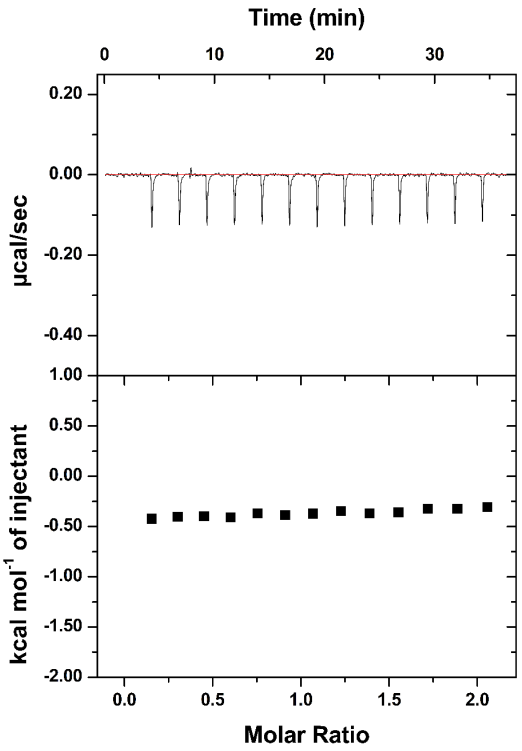

Figure 2. Evaluation of Sertraline/TCTP interaction by Isothermal Titration Calorimetry (ITC). Representative ITC thermogram at 25°C (top) and integrated heat data (bottom) of Sertraline titration (syringe) into TCTP (cell) as a function of the molar ratio of drug to protein.

TCTP-drugs interaction from SPR and BLI techniques

So far, NMR and ITC failed to detect the ~50 µM interaction described by Amson and co-workers by a single-technique SPR experiment[17]. Therefore we engaged in using SPR, but also Bio-Layer Interferometry (BLI) to validate and revisit TCTP-drugs interaction in our hands. Both methods are label-free and widely used to study the interactions of drugs (including proteins, nucleic acids, sugars, and small molecules) with analytes[46,47] and in the best case, can provide binding affinities. We carefully setup the experiments to be as close as in the reference experiment [17]. TCTP was immobilized on the surface while analytes (sertraline or thioridazine) were flowed past the surface via a micro-fluidic system (SPR) or via stirring the microplate (BLI).

The analyte recognition by the ligand induces a small change in the refractive index and in the layer thickness at the surface/solution interface, which can be quantified with high precision. The variation of the signal versus time (sensorgram) (see Figure 3) reflects the kinetics and the equilibrium of the interactions. Qualitatively, the SPR sensorgrams obtained for the two drugs in our study and the reference study [17] were similar. Indeed, the signals recorded by SPR, but also by BLI, increased with the analyte concentration without ever saturating in the concentration range tested, and this despite the higher maximal concentrations used in our study (500 µM versus 100 µM). This is likely due to a very low affinity of the analyte for the ligand (TCTP) immobilized on the surface.

Nevertheless, an estimation of the dissociation constant could be deduced with the response at the steady state (R_{eq}). The adsorption isotherm was fitted with the 1:1 interaction mode (see Figure 3C) and the resulting equilibrium dissociation constants (see Table 1) obtained from the SPR measurement were estimated to K_D = 1.2 mM and K_D = 1.0 mM for sertraline and thioridazine respectively (see Figure 3C). A concordant value was obtained from the BLI sensorgram for sertraline, K_D = 1.4 mM (Figure 3D). In absence of saturation, the Kd values given in this study should only be considered as estimations.

In our hands, the two different BLI and SPR techniques clearly revealed that a single very weak (~mM) binding mode was sufficient to fit the data for both sertraline and thioridazine and the experimental data did not require to take into account stronger ~30-50 µM affinity mechanisms that would be visible at the lower concentration range (below 100 µM), thus contradicting the reference experiments [17]. Despite similar raw data between the two studies, including the non-saturating conditions at the steady state (R_{eq}), we used here 8 concentrations values (compared to 3), as required by common practice (i.e. at least 5-7 different analyte concentrations from 0.1*K_D to 10*K_D) and fully interpreted the SPR signals. In addition, our sensorgrams were totally devoid of the strong injection peaks that clearly obscured the kinetic part of the SPR curves in the reference experiment [17] making our conclusions even stronger. This part of the sensorgram is central during the mathematical treatment of the kinetic analysis method since the kinetic parameters are obtained from the curvature before reaching the plateau. Note that the authors used the kinetic analysis method to derive the reported ~30-50 µM affinity value [17]. Note also that only 10% of the signal was fitted in the reference experiment (4 RU for a signal near 40 RU at 100 µM for sertraline) [17], in spite of the subtraction of the reference flow cell, which already allowed the correction of the running buffer. As a consequence, 90% of the visible SPR signal was corrected, but not interpreted, by the authors while only a small 10% fraction of the total signal was interpreted as the binding process. For thioridazine, it is more problematic as the correction factor is superior to the experimental data (65 versus 40). In contrast here we interpreted the major SPR signal to a ~mM Kd range TCTP/drug interaction without the need to introduce a second binding mode to properly fit the raw data.

Another observation is the unexpected intense signal recorded by SPR and BLI for the two analytes of low molecular weight (thioridazine 370.5 Da, sertraline 306.2 Da). Indeed, with the quantity of TCTP immobilized on the SPR sensor chip (5400 RU) and the Wilson formula [48], a maximum response around 100 RU was expected. In this case after fitting (Table 1), the maximal response was much higher (R_{max} = 727 RU and R_{max} = 1489 RU for sertraline and thioridazine, respectively). This large difference could be explained by an alteration of the protein structure which might modify the hydrodynamic radius and so the refractive index increment (RII) of the complexes. The modification of the tridimensional structure of TCTP also induces a RII deviation of the TCTP/analyte complex from the sum of the RII of individual entities. Indeed, conformational changes of an immobilized receptor have an impact on the SPR detection of low molecular weight molecules, as seldom described in the literature [49,50,51,52,53].

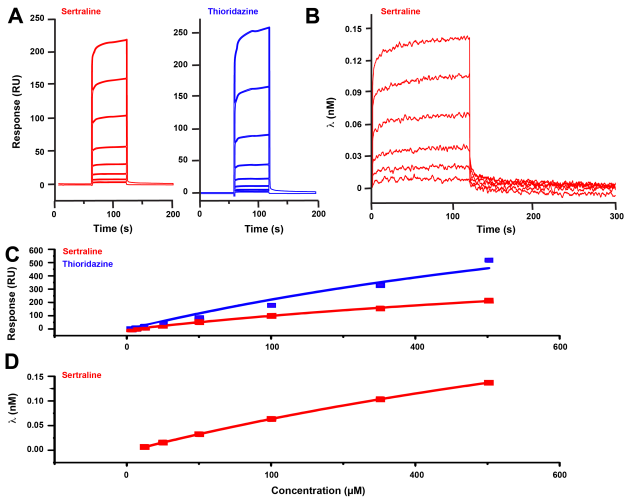

Figure 3. Sensorgrams for the TCTP interaction with sertraline (red) or thioridazine (blue) by SPR (A) or BLI (B). The concentrations for the experiments were 6.25, 12.5, 25, 50, 100, 200, 350, 500 µM and 25, 50, 100, 200, 350, 500 µM for SPR and BLI experiments respectively. The sensorgrams correspond to double subtracted data (blank and reference subtraction). Adsorption isotherm (square) and fitting curve (line) using a 1:1 Langmuir interaction model for the interaction of TCTP with sertraline (red) or thioridazine (blue) by SPR (Panel C) or BLI (Panel D).

Table 1. Thermodynamic dissociation constants (Kd) and the maximal response (Rmax) obtained by the Langmuir fitting of the SPR and BLI equilibrium response.

		K_D (mM)	R_{max}
SPR	Sertraline	1.2 ± 0.2	727 ± 71
	Thioridazine	1.0 ± 0.1	1489 ± 124
BLI	Sertraline	1.4 ± 0.1	0.53 ± 0.02

Drugs effect on TCTP thermal stability by Thermal Shift Assay (TSA)

The melting temperature of proteins is a parameter of interest in characterizing ligand-effect on protein stability but also in drug-screening strategies. Indeed, ligand binding is generally associated with an increase of the denaturation temperature of proteins due to increased stability conferred by the intermolecular interaction[54]. In this scope, Thermal Shift Assay (TSA) is a method of choice lying on the SYPRO Orange fluorescent probe which is a binder of solvent-exposed hydrophobic segments of proteins, over-represented in temperature-induced protein denaturation states. Here, with the aim to further describe the strong SPR and BLI signals and the TCTP-drugs interactions, we measured the melting temperature of TCTP in presence of sertraline or thioridazine at drug concentrations between 0 to 500 µM (Figure 4). Experimental data were of excellent quality, as exemplified for a range of sertraline concentrations and the corresponding opposite derivatives of TCTP denaturation curves (Figure 4A). We could observe a slight response (+0.5°C) of TCTP to the presence of sertraline and thioridazine near 50 µM ligand concentration. Nevertheless, this slight increase of the melting temperature was also found for unrelated control proteins (Figure 4D) such as citrate synthase (CS, +0.4°C) and the response was even stronger for CPR protein (hCPR) (+1.4°C), which is an evidence for non-specific effect of sertraline. This lack of specificity was confirmed for higher ligand concentration, with TCTP and all control proteins exhibiting the same marked down trend upon inspection of melting temperatures in ligand concentrations ranging from 100 µM to 500 µM. Consequently, TSA failed to demonstrate specific interactions between TCTP and sertraline or thioridazine at concentrations below 100 µM.

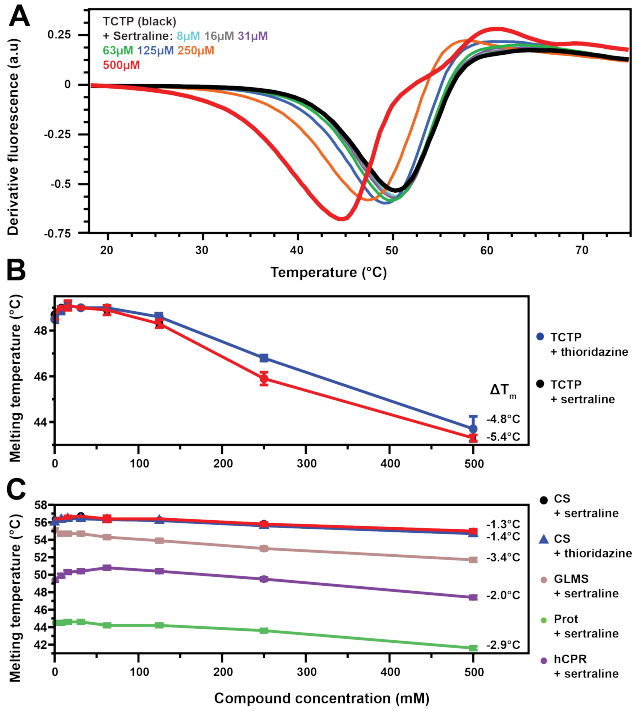

Figure 4. (A) Opposite of the derivative of the thermal denaturation curve of TCTP in the presence of increasing sertraline concentrations. The melting temperatures measured for TCTP (panel B) and four control proteins (panel C) for increasing compound concentrations are also shown. The difference ΔTm in the melting temperature between 0 and 500 µM compound is also reported. TSA experiments were done by applying a temperature gradient from 10°C to 95°C at a rate of 3°C.min^{-1} in 10 mM HEPES pH 7.4, 150 mM NaCl, 2 mM TCEP, 5 mM EDTA and 2.5 % DMSO.

A unified picture of TCTP-drug interactions

Taken together, the NMR, ITC, SPR, BLI and TSA methods were consistent with very weak (~mM) TCTP/drugs interactions, in contrast to the previous study [17]. Data obtained from the five techniques are compatible with a simple model in which TCTP protein is essentially free and monomeric at drug concentrations lower than 100-200 µM. At higher drug concentrations, the drugs have destabilizing effects leading to formation of aggregates or denatured protein, as revealed from the TSA-derived lower melting temperatures, the reduced intensity in NMR spectra and the very strong SPR and BLI signals. In contrast, NMR and ITC signals were less sensitive to drug-induced protein destabilization and both, unambiguously, did not detect any TCTP-drug interaction below 200 µM drug concentration.

NMR/MS characterization of TCTP upon Plk-1 mediated phosphorylation.

As pointed out in the introduction, TCTP phosphorylation strongly perturbs protein-protein and protein-ligand TCTP interaction profiles. Yet the impact of phosphorylation on TCTP structure/dynamics is unknown. Therefore we next aimed at characterizing the structure/dynamics of phosphorylated TCTP and at assessing putative consequences for the interaction with the drug sertraline.

^{15}N (or ^{15}N-^{13}C) labeled phosphorylated TCTP was prepared by incubating ^{15}N (or ^{15}N-^{13}C) TCTP (2 hours, 30°C) with pre-activated Plk-1 followed by purification on a Size Exclusion Chromatography (SEC) S75 column. Mass Spectrometry (MS) MALDI-TOF spectra collected on native TCTP and pTCTP samples contained each a single monocharged peak with a mass difference of 82.4 Da. This is consistent with a TCTP phosphorylation yield of 100% with a single phosphoryl group addition per protein copy. ^{15}N SOFAST HMQC spectra of TCTP and pTCTP were rather similar, although a subset of ~10 crosspeaks showed significant chemical shift perturbations (see Figure 5). We resorted to triple resonance experiments to fully assign pTCTP. The residues most affected upon phosphorylation were in the vicinity of residue S46 (Figure 5B) but also around residue F83. However no significant chemical shift variation was observed for other potential Plk-1 phosphorylation sites such as S64 and T65. The chemical shift perturbation around residues F83 was interpreted as a perturbation of the monomer/dimer equilibrium upon phosphorylation (*vide infra*). When interpreted in light of the MS results, these NMR data demonstrate that under our conditions the Plk-1 mediated phosphorylation of TCTP in vitro led to the complete phosphorylation of the primary Plk-1 phosphorylation site residue S46 but not of S64/T65, consistent with previous observations [32].

Since S46 phosphorylation impacts TCTP primary structure, it may lead to changes in the TCTP structure/dynamics relevant for the regulation of biological interactions [24]. The very similar ^{15}N SOFAST HMQC spectra for native TCTP and pTCTP states indicate that the conformational/dynamic change was restricted to the region around the phosphorylation site, in an otherwise unmodified structure. To further characterize the protein dynamics, we measured ^{15}N relaxation rates and $\{^1H\}$-^{15}N heteronuclear NOE parameters to assess global and internal mobility for TCTP and pTCTP (Figure 5C). The average ^{15}N R_2/R_1 ratio measured on the structured part of a folded protein is directly related to the global tumbling of the protein, recapitulated in the correlation time τ_c. This parameter was 9.19 ± 0.07 ns for native TCTP and 9.09 ± 0.07 ns for pTCTP under the same experimental conditions, indicating a limited decrease in the global rotational mobility of the protein upon phosphorylation, in line with a perturbation of the monomer-dimer equilibrium or a change in loop conformational excursion. Within the internal flexible TCTP loop, we observed a significant increase in R_2/R_1 ratio and $\{^1H\}$-^{15}N heteronuclear NOE values for residues D45-S46-L47, which is consistent with a moderate change in dynamics around the phosphorylation site S46. The perturbation of local dynamics in the loop was further supported by the presence in the ^{15}N SOFAST-HMQC spectrum of p-TCTP of additional peaks of weak intensity in the vicinity of the major resonances for residues 52 to 55 and 63 to 65. These peaks were absent in the spectrum of native TCTP. The additional crosspeaks in pTCTP hence reveal a complex conformational energy landscape around residues 52 to 55 and 63 to 65 to accommodate long living sub-states not existing or undergoing fast exchange with the major conformational ensemble (Figure 5A). pS46 phosphorylation therefore led to a change in local dynamics in the loop around pS46 but also remotely at positions 52 to 55 and 63 to 65.

SAXS description of pTCTP oligomeric state and motion amplitudes.

The previous NMR relaxation analysis gave access to local dynamic change but not to the amplitude of the motion. By contrast, Small Angle X-ray Scattering (SAXS) is not sensitive to motion timescale but is an excellent proxy to probe the spatial excursion of conformational ensembles in flexible proteins [55]. We therefore collected Size-Exclusion Chromatography (SEC)-SAXS data, yielding scattering curves of high quality (Figure 5D, 5E, 5F) further used to extrapolate the intensity at origin I(0), the molecular weight (MW) and radius of gyration (Rg) of native and phosphorylated TCTP reported in Table 2. MW was computed to 31.5 kDa, corresponding to the population-averaged molecular weight between TCTP monomer and dimer as described in detail in the previous study [24]. Upon phosphorylation, MW increased to 36.1 kDa, elution volume decreased from 30.6 to 29.8 mL and the Rg increased from 21.4 Å to 23.4 Å, fully consistent with phosphorylation-induced increase in the population of dimer, in line with NMR chemical shift perturbations around residue F83 (*vide supra*). Changes in protein dynamics upon phosphorylation were assessed by representing SAXS curves with respect to the dimensionless Kratky formalism. In the subsequent Kratky plot (Figure 5F), we could observe that signal returns to baseline around q.Rg at 4.5-5 which means that the proteins are globally well-folded. However, the experimental plot deviates from the theoretical curve predicted for a globular structure (grey curve), consistently representing the elongated conformations from the highly flexible 30 amino-acid internal loop that represents about 20% of TCTP sequence. Comparatively, Kratky plots for TCTP and pTCTP were very similar, demonstrating that phosphorylation does not strongly modify the amplitude of loop motion. As a conclusion from the NMR and SAXS analysis, phosphorylation of S46 did not modify the 3D structure of the protein and had detectable, but limited, impact on the local mobility in the long internal loop and on protein self-association.

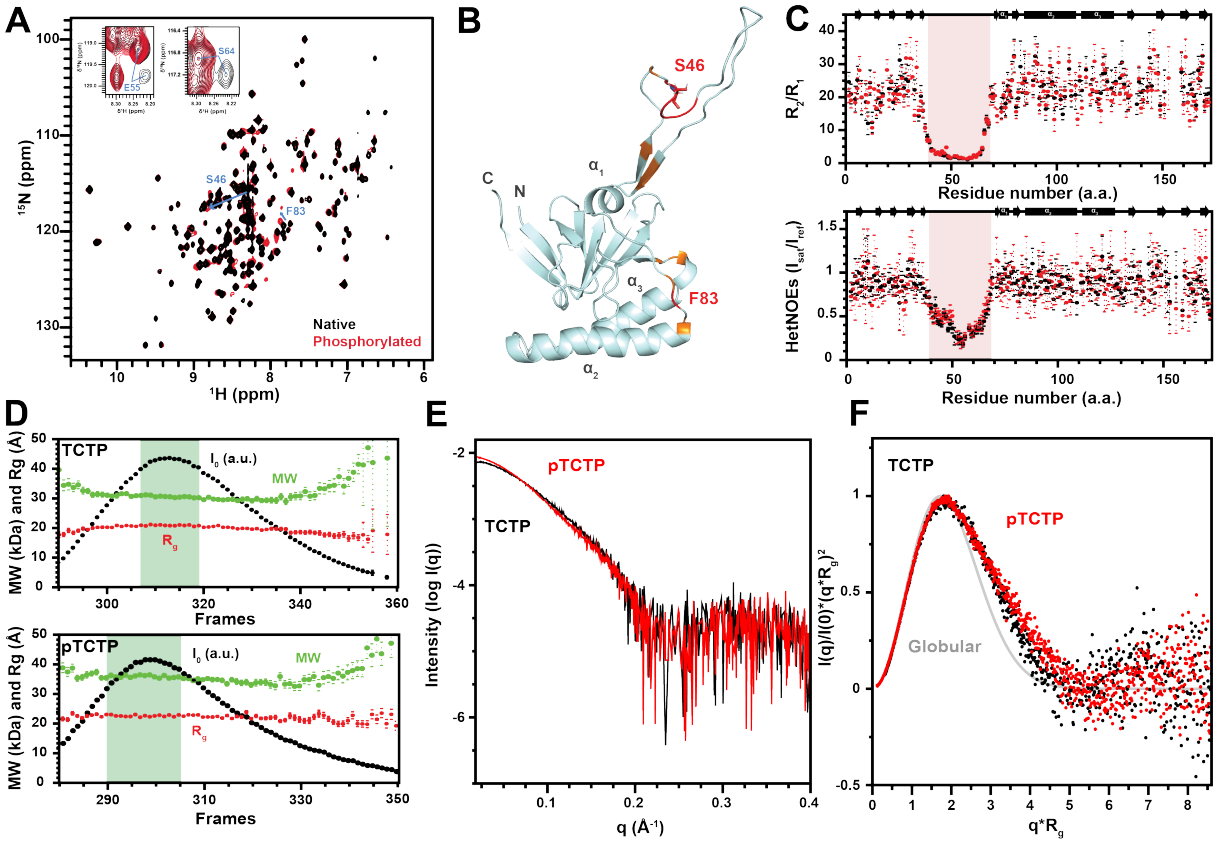

Figure 5. Comparison of TCTP and phosphorylated TCTP (pTCTP). (A) Overlay of ^{15}N SOFAST-HMQC spectra of 100 μM ^{15}N labeled TCTP collected before (black) and after (red) phosphorylation and after buffer exchange to 50 mM HEPES pH 7.4, 150 mM NaCl, 2 mM TCEP. The spectra were collected at 950 MHz and 25°C. The most shifted resonances are labeled. (B) The chemical shift perturbations (CSP), calculated as sqrt($\Delta\delta H^2$+ 0.144* $\Delta\delta N^2$) where $\Delta\delta$H and $\Delta\delta$N are the differences in chemical shifts (ppm) for ^{1}H and ^{15}N, respectively, upon phosphorylation, are mapped on the structure of TCTP (panel B). Residues with CSP > 0.1, 0.1 > CSP > 0.05, CSP < 0.05 are colored red, orange or cyan respectively. (C) The ratio of the ^{15}N R_2 and R_1 relaxation parameters and {^{1}H}-^{15}N heteronuclear NOE values for both native (black) and phosphorylated (red) TCTP are shown. {^{1}H}-^{15}N heteronuclear NOE values were calculated as the ratio of the cross-peak intensities in presence (Isat) or absence (Iref) of ^{1}H irradiation. The experimental data were collected at 950 MHz and 25°C in 50 mM HEPES pH 7.4, 150 mM NaCl and 1 mM TCEP buffer. (D-E-F) SEC–SAXS results for TCTP and pTCTP. The scattering intensity I_0, the molecular weight (MW) and the radius of gyration (Rg) are shown for the different frames along the SEC dimension. The green areas correspond to the frames used for integration and calculation of the I(q)=f(q) scattering curve (panel E). Panel F represents the normalized dimensionless Kratky plots for both proteins, as well as the prediction for a globular protein (gray). The buffer for SAXS analysis was 50 mM EPPS pH 8, 50 mM NaCl and 2 mM TCEP and the SAXS curves were collected at 20°C.

Table 2. Small Angle Scattering results for TCTP and phosphorylated TCTP (pTCTP)

	SEC Elution Time (min)	Combined data frames	Rg (Å)	I(0) (cm^{-1})	D_{max} (Å)	MW based on the Volume of Correlation (US-SOMO)	MW from sequence (kDa) for a monomer/dimer
TCTP	30.6	307-319	21.5 +/- 0.1	0.0083 +/- 0.0001	74	31.6	19.8 / 38.6
pTCTP	29.8	289-305	23.4 +/- 0.1	0.0093 +/- 0.0001	81	36.6	19.9 / 38.8

Attempt to detect pTCTP-sertraline interaction by NMR

In order to assess if S46 phosphorylation could impact (increase) TCTP-sertraline interaction, we recorded ^{15}N SOFAST-HMQC spectra of isolated phosphorylated TCTP and upon successive addition of sertraline, up to 550 µM. The interaction was also monitored from the sertraline side by recording 1D ^{1}H NMR spectra (Figure 6). As observed for native TCTP, no significant spectral change was visible for sertraline concentrations up to 200 µM and larger concentrations also induced a global decrease in signal intensity for most residues in the folded state. This indicates that S46 phosphorylation had no significant impact on the interaction between TCTP and sertraline.

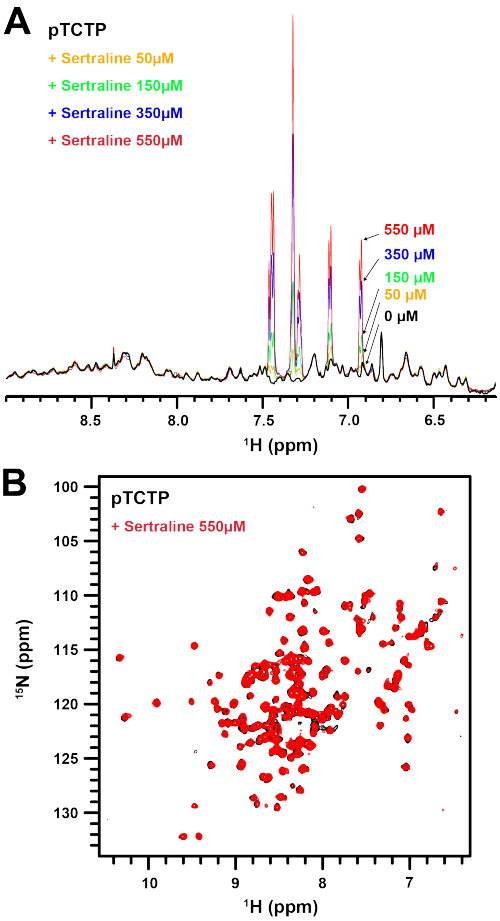

Figure 6. Impact of phosphorylation on TCTP interaction with sertraline. A 30 µM ^{2}H-^{15}N-^{13}C labeled pTCTP was incubated in 150 mM NaCl, 50 mM HEPES pH 7.4, 2 mM TCEP, 0.5 mM EDTA, 5% DMSO with 95% / 5% H_2O / D_2O. The desired amount of dried sertraline was added to the sample to reach 50, 150, 350 or 550 µM concentration. (A) Series of water-suppressed 1D ^{1}H spectra acquired at increasing sertraline concentration. At 550 µM, a global ~30% decrease in intensity was observed on pTCTP while at lower concentrations the protein spectra remained unchanged. (B) Overlay of the ^{15}N SOFAST-HMQC spectra acquired at 0 µM (black) and 550 µM (red) sertraline concentration. The spectra were scaled at similar intensity levels to account for the ~30% intensity change.

Discussion

The antidepressant sertraline has been introduced as a TCTP inhibitor and was repositioned in Acute Myeloid Leukemia. The access of this molecule to clinical trials against cancer was greatly facilitated since the Selective Serotonin Reuptake Inhibitors (SSRI) molecule was already approved to treat depression in many countries. A first set of phase I/II clinical trial carried out under mono-therapy led to promising results but with adverse side effects at the dose used[34]. A current strategy is a bi-therapy combining ara-C with low dose of sertraline with a phase I/II clinical trial started in 2014[34].

We intended to characterize TCTP-inhibitor interactions for further rational drug design to limit sertraline side effects. Based on data, we conclude that sertraline and thioridazine do not directly bind to TCTP in the submillimolar affinity range and that the two drugs lead to protein destabilization at high drugs concentrations. In this way, our results challenge previously reported data that claimed ~30-50 µM affinity range for the two drugs, and even submicromolar (0.1- 0.2 µM) "when using highly purified TCTP" [17]. Our extensive multi-technique study reinforces the need to use complementary techniques, not only to validate protein-ligand interactions but also to provide a complete picture of the molecular interaction. The validation of protein-ligand interaction is central when considering the mode of action of drugs, notably when used in clinics, but also to build on medicinal efforts in structure-based rational drug design approaches. Here, to the best of our knowledge, the direct interaction of TCTP with the two drugs was not reproduced, nor validated by other techniques since the initial report [17] and our new data, combined with a critical analysis of the published SPR raw data, allowed building a complete picture of TCTP-drugs interactions: namely, a drug-induced strong protein destabilization occurring with an apparent ~mM Kd range. Our integrative view of TCTP-drug *in vitro* interactions established that rational drug design based on isolated TCTP, phosphorylated at position S46 or not, is not viable and leads us to reinterrogate the mode of action of the drugs.

It is well established that in different tumor cell types the drugs sertraline and thioridazine reduce TCTP levels and restore p53 levels, both contributing to restore sensitivity of tumor cells to apoptosis. The suggested mode of action is that by directly interacting with TCTP, the two drugs prevent TCTP to bind and activate the E3 ligase MDM2, hence reducing p53 proteasomal degradation and restoring p53 levels [17]. This is supported by *in vitro* ubiquitination assays carried out on p53 via MDM2 which unambiguously showed that sertraline and thioridazine (~10 µM) prevent TCTP from inhibiting the MDM2-mediated ubiquitinylation of p53 [17]. In light of the current work, a mechanism by which the drugs directly bind to isolated TCTP to prevent TCTP to interact with MDM2 at 10 µM compound concentration is likely ineffective. Therefore alternative mechanisms, involving for example drugs interactions with heterodimeric protein complexes or with other protein partners, need to be invoked and be experimentally evaluated in the future.

In a more general scope, the use of SSRIs including sertraline (Zoloft) is associated with a reduced risk of bladder cancer[56], heptacellular carcinoma[57], ovarian cancer[58], colorectal cancer [59] and with an extended survival in several cancers[60,61]. Using animal, tissues or cellular models, numerous studies have pointed out the anti-tumoral properties of sertraline although not converging to a unified mechanism [62,63,64,65,66,67,68,69]. The anti-tumoral properties of thioridazine have also been extensively supported by several independent studies [70,71,72,73,74,75] with ligand concentration down to 10 µM. Sertraline and thioridazine are well-known polypharmacological ligands of integral membrane receptors with primary targets at the sodium-dependent serotonin transporter [76] for sertraline and at the Dopamine G-Protein Coupled Receptors for thioridazine [77,78]. The latter

drug is a strong antagonist of the dopamine receptor DRD2 with Ki in the 10-20 nM range while antidepressants such as sertraline (Ki in the 10-20 µM range) are also weak competitive DRD2 antagonists [79,80]. To this regard, the role of DRD2 in tumor fate is well-established[81]. For instance, transient DRD2 knockdown in HCT116 colon cancer cells showed reduced viability and activation of the integrated stress response[82]. The anti-tumor activity of thioridazine mediated by DRD2 inhibition has also been shown in breast cancer cells [83]. Overall, thioridazine used as a DRD2 blocker in the context of cancer has been proven to be promising for the development of related anti-cancer drugs [75,83,84] and represents a plausible top level signaling layer to explain the anti-tumor properties of the drugs. As a central kinase integrating extracellular signals and environmental inputs, such as energy, nutrient, oxygen and growth factor signals, the mTOR complex regulates cell growth and protein synthesis[85] and is part of the downstream layers under regulation of DRD2 or, more generally, GPCR and integral membrane receptor. Interestingly, sertraline has been shown to inhibit mTOR pathway[62,63] and thioridazine also suppresses tumor growth activity by targeting the PI3K/Akt/mTOR/p70S6K[70,86], the αvβ3/FAK/mTOR [87] or the VEGFR-2/PI3K/mTOR [88] signaling pathways. Back in the scope of TCTP, there is now strong evidence that TCTP is up-regulated at the translational level by the mTOR complex [22,89,90,91,92]. Accordingly, TCTP levels are controlled through the mTOR pathway by environmental factors such as serum[89,93] and hence other pharmacological compounds regulating mTOR might potentially also regulate TCTP. Seducing as much as plausible, a mechanism by which sertraline and/or thioridazine could indirectly control TCTP, and ultimately p53 levels through mTOR signaling pathways would deserve consideration for further functional studies.

As a conclusion, we revisited here in-depth the in vitro interactions between the cancer drug target TCTP and the two well-known drugs sertraline and thioridazine. We believe that our new results will foster novel investigations to assess the contributions of TCTP-dependent and TCTP-independent pathways to the anti-cancer effects of the two drugs with well-defined actions on extracellular membrane receptors.

Experimental Section

Expression and purification of the human TCTP

The details of TCTP protein production and purifications were given elsewhere[24] for ^{15}N and/or ^{13}C labeled TCTP protein. To produce perdeuterated ^{2}H-^{15}N-^{13}C labeled TCTP, we progressively adapted bacteria to increasing D_2O / H_2O ratio from 0%, 25%, 50%, 75% to 100% in M9 minimal medium containing $^{15}NH_4Cl$ and ^{13}C-α-D-glucose. We first cultured bacteria in 5 mL M9 medium with 0% D_2O and when the cultured reached OD_{600} ~ 0.6, we inoculated the 5 mL 25% D_2O medium at OD_{600} ~ 0.05 and we repeated the operation to reach 100% D_2O.

The phosphorylation of TCTP was achieved by the addition of a pre-activated Plk-1 (generously provided by the protein production facility of the Institut Curie, Orsay, France) to ^{15}N or ^{2}H-^{15}N-^{13}C labeled TCTP in the following buffer: 40 mM HEPES pH 8, 20 mM $MgCl_2$, 5 mM ATP, 1 mM EDTA and 1 mM DTT at 30°C. The TCTP to Plk-1 molar ratio was between 1000:1 and 500:1 to reach complete phosphorylation within two hours. At the end of the reaction, 100 mM EDTA was added to the reaction buffer to sequester the Mg^{2+} ions that bind TCTP. The phosphorylated protein was further purified on a Superdex 75 10/300 GL column (GE Healthcare life sciences) in the desired buffer.

To evaluate TCTP/sertraline interaction by Isothermal Titration Calorimetry (ITC), a pDEST17 expression vector containing TCTP (residues 1 to 172) was kindly provided by Dr. Palma Rocchi (CRCM, Marseille) and was overexpressed from E.coli BL21 plysS(DE3). The produced TCTP protein (bearing a N-terminal 6 x histidine tag) was purified on a FPLC system (Akta PURE, GE Healthcare life sciences) using affinity chromatography (GE Healthcare, HisTrap HP) followed by a size exclusion step (Superdex 200 10-300 GL, GE Healthcare life sciences) in 50mM phosphate pH 7.8, 200mM NaCl.

Nuclear Magnetic Resonance (NMR) Spectroscopy

Unless specified, NMR spectroscopy measurements were performed at 25°C in the following buffer: 50 mM HEPES pH 7.4, 150 mM NaCl, 2 mM TCEP in 95% / 5% H_2O/D_2O. Measurements were performed using Bruker AVIII 950 MHz and 800 MHz spectrometers equipped with a TCI cryoprobe. 2D ^{1}H-^{15}N correlation spectra were collected using the SOFAST-HMQC scheme[94]. Sequence-specific backbone assignment of human non phosphorylated TCTP was already available[24,25] and the assignment of the phosphorylated TCTP was completed by collecting additional triple resonance experiments using the BEST-TROSY approach[95,96] as implemented in the NMRLib package [97]. All NMR data, except ^{15}N relaxation measurements, were processed with Topspin 3.5 (Bruker) and analyzed with CCPNMR software[98].

Titration experiments with sertraline and thioridazine (Sigma-Aldrich) were carried out as follows: the molecule was weighted, dissolved in methanol, and aliquots of the required amounts were lyophilized. The purity and structural integrity of the molecules were verified by NMR. This allowed addition of the desired amount of compound to TCTP solution without changing DMSO concentration nor dilute the protein solution. This protocol was thoroughly tested for the recovery and dissolution of the molecule into the buffer by monitoring the ^{1}H signals from the molecule in the final buffer. The proper removal of methanol during lyophilization was also confirmed by the absence of the methanol signal in the resulting ^{1}H NMR spectra.

The Saturation Transfer Difference (STD) experiment was carried out at 8°C using a Bruker AVIII 800 MHz spectrometer with unlabeled TCTP protein at 15 µM and sertraline molecule at 125 µM in the following buffer: 10mM HEPES pH 7.4, 150 mM NaCl, 3 mM EDTA, 2.5% DMSO in 97.5% / 2.5% H_2O/D_2O. Selective ^{1}H saturation before collecting the ^{1}H spectrum was achieved using a 50-ms Gaussian selective pulse train of 2 s. Water signal was suppressed using the excitation sculpting method. The reference experiment was obtained upon off-resonance saturation at -62.5 ppm and compared to the on-resonance spectrum recorded after saturation at 0 ppm, a region which covers protein signals but which does not include signals from the free sertraline molecule.

Relaxation experiments were performed using a Bruker AVIII HD 950 MHz spectrometer at 25°C with a ^{15}N-labeled phosphorylated and non-phosphorylated TCTP at 100 µM protein concentration under the same buffer conditions and processed using NMRPipe software [99] and in-house scripts. The ^{15}N relaxation experiments were recorded in interleaved pseudo-3D fashion to attenuate the effects of sample and/or conditions changes during the collection time. The ^{15}N R_1 values were determined from series of 2D ^{1}H-^{15}N correlation spectra recorded with the following delays (ms): 10, 3000, 200, 2500, 400, 2000, 600, 1500, 800, and 1000 (in this order). The ^{15}N R_2 values were determined with different relaxation delays (ms): 13.7, 137.6, 27.5, 82.6, 0, 41.3, 68.8 and 55 (in this order). $\{^{1}H\}$-^{15}N heteronuclear NOE experiments were recorded using one reference and one proton-saturated 2D ^{1}H-^{15}N correlation experiment. ^{1}H saturation was achieved by a train of 120°

pulses. ^{15}N R_1, R_2 and {^1H}-^{15}N heteronuclear NOE were recorded with an interscan delay of 5, 3.5, and 4.8 s, respectively. Intensities from R_1, R_2 and {^1H}-^{15}N heteronuclear NOE experiments were extracted using the nlinLS routine in NMRPipe [99] and R_1 and R_2 values were obtained by fitting intensities with a two-parameter exponential model with the modelXY tool in NMRPipe. Further analysis of ^{15}N relaxation parameters and {^1H}-^{15}N heteronuclear NOE in terms of rotational diffusion tensor was achieved by using TENSOR2 software[100].

Thermostability measurements by fluorescence-based thermal shift assay (TSA).

TSA was used to monitor the TCTP thermal denaturation in presence or not of thioridazine or sertraline. To measure the effect of sertraline and thioridazine on TCTP melting temperature, we mixed the stock solution of TCTP and a 40 mM sertraline stock solution in 100% DMSO to reach a final sample containing 2.5 µM TCTP in 10mM HEPES pH 7.4, 150 mM NaCl, 2 mM TCEP, 5 mM EDTA at 2.5% DMSO with the desired concentration of ligand. The samples were prepared carefully to ensure identical DMSO concentrations in all the samples. To test the effect of sertraline on the melting temperatures of other proteins, we used the human NADPH-dependent cytochrome P450 reductase (hCPR)[101], the *E. coli* GlmS[102], citrate synthase and a fourth protein. Reaction mixtures were made in duplicate in a MicroAmp Optical 384-well reaction plate at a final volume of 10 µL and each experiment was repeated at least twice independently. Experiments were carried out in 7900HT Fast Real-Time PCR System (Applied Biosystems) with a temperature gradient in the range of 10–95°C at 3°C/minute.

Surface Plasmon Resonance (SPR)

All SPR measurements were performed at 25 °C in a two flow cell Biacore T200 instrument (GE Healthcare) with a CM5 sensor chip. For most immobilization approaches, the surface is activated with a mixture (1:1 v/v) of 1-ethyl3-3-(3-dimethylaminopropyl)carbodiimide (EDC) at 0.4 M and N-hydroxysuccinimide (NHS) at 0.1 M during 7 minutes at 10 µL/min. Then the protein was injected, on flow cell 2 only, on acetate buffer, pH 4.6, at 100µg/ml and 10µL/min. To finish the two flow cells were deactivated with ethanolamine-HCl 1M during 7 minutes at 10µl/min. At the end, around 5400 RU of TCTP was immobilized on the active flow cell 2. Sertraline and thioridazine solutions with different concentrations were injected for 60 seconds at 80µL/min and the flow cells were then rinsed with the running buffer (10 mM HEPES, 3 mM EDTA, 150 mM NaCl, 0.005% P20, 5% DMSO) during 3 minutes. The signal recorded on the reference (activated and deactivated flow cell) channel 1 was subtracted from the signal of the sample channels 2 by applying double-referencing procedure: correction of the device drift and of the refractive index difference between the running buffer and injected solutions [103] and a solvent correction was performed before and after each analyte. The value of the signal was measured 4 s before the end of the analyte injection and the adsorption isotherm was fitted with the 1:1 interaction mode (Langmuir isotherm). The reported values are the means of representative independent experiments, and the errors provided are standard deviations from the mean. Each experiment was repeated at least two times.

Bio-layer interferometry (BLI)

Bio-layer interferometry experiments were performed using sensors coated with amine reactive second generations (AR2G sensors) purchased from Forte Bio (PALL). Prior to use, they were immersed for 10 minutes in water before functionalization to dissolve the sucrose layer. Then the sensors were functionalized by TCTP with the same procedure as for the SPR experiments. The functionalized sensors were next dipped in the sertraline solution at different concentrations for 2 minutes interspersed by a rinsing step in the buffer solution for 3 minutes. Reference sensors without TCTP immobilization were used to subtract the non-specific adsorption on the activated-deactivated AR2G layer. The value of the signal was measured 4 s before the end of the analyte injection and the adsorption isotherm was fitted with the 1:1 interaction mode (Langmuir isotherm).

Isothermal titration calorimetry.

His-tagged TCTP and sertraline were diluted in the ITC buffer 50mM phosphate pH 7.8, 200mM NaCl complemented to a final 2% DMSO concentration. ITC titrations were performed on a MicroCal ITC200 microcalorimeter (GE Healthcare) at 25 °C and at 35°C using 13 injections of the titrant (1 mM sertraline in the syringe) into the analyte (100 µM TCTP in the cell). A first small injection (0.2 µl) was included in the titration protocol in order to account for cell/syringe premix and/or remove air bubbles trapped in the syringe prior titration. Raw data were scaled to the baseline using MicroCal Origin 9.1 (Origin Lab).

SAXS data collection and analysis

SAXS experiments were performed at the SWING beam-line at the SOLEIL synchrotron (Saint-Aubin, France) using an online high-performance liquid chromatography (HPLC). All experiments were performed at 20 °C. The SAXS data were recorded using an EigerX 4M detector at a distance of 2 m. For phosphorylated and non-phosphorylated TCTP, a stock solution was prepared at a final concentration of 500µM (9.35 mg/ml). A volume of 75 µL protein samples was injected into a size exclusion column (Superdex 200-10/300-) and eluted directly into the SAXS flow-through capillary cell at a flow rate of 0.5 ml/min. The overall SEC-SAXS setup has already been described in previous works [104,105]. The elution buffer consisted of 50 mM EPPS pH 8, 50 mM NaCl and 2 mM TCEP. 900 SAXS frames were collected continuously during the elution at a frame duration of 1.99 s and a dead time between frames of 0.01 s. 180 frames accounting for buffer scattering were collected before the void volume. Data reduction to absolute units, buffer subtraction and averaging of identical frames corresponding to the elution peak frame were performed with the softwares FOXTROT[104] and US-SOMO[106]. US-SOMO was also used to estimate the molecular weight (MW) based on the Volume of correlation[107]. Data analysis to obtain I(0), Rg, and Dmax were conducted with the PRIMUS software from the ATSAS Suite[108]. Scattering patterns I(q) are also shown as dimensionless Kratky plots ((q.Rg)2.I(q)/I(0) versus q.Rg), to assess the globularity and the flexibility in the two proteins. Typically, a globular, structured protein exhibits a pronounced maximum (bell-shaped curve), whereas a random chain (for example, an unfolded protein) will plateau[55].

Acknowledgements

We would like to thank Vincent Guérineau and Nadine Assrir for helpful assistance in mass spectrometry measurements and analysis and in protein production/purification respectively. We also thank the synchrotron facility SOLEIL (St. Aubin) for allocating beam time (proposal 20181072) and its dedicated staffs for technical help with the beamline SWING as well as the Nanobio-ICMG platform (FR 2607) for providing facilities for surface plasmon resonance and BioLayer Interferometry measurements. We thank the protein production facility of the Institut Curie for providing the purified kinase Plk1.

Funding

This work was supported by the CNRS (Centre National de la Recherche Scientifique), by the French Infrastructure for Integrated Structural Biology (https://www.structuralbiology.eu/networks/frisbi,

grant number ANR-10-INSB-05-01). This work is supported by the LabEx LERMIT (Grant ANR-10-LABX-33) and by the “IDI 2016” project funded by the IDEX Paris-Saclay ANR-11-IDEX-0003-02 as a master and PhD fellowship to F.M. Financial support from the IR-RMN-THC Fr3050 CNRS for conducting the research is gratefully acknowledged.

Supplementary Material

The following are available online at XXXXXXX,

Figure S1: Binding assay of TCTP to Bcl-xL and reversion with ABT-737.

Figure S2: Effect of DMSO on TCTP structure.

Keywords: TCTP • Sertraline • Thioridazine • NMR • SPR

References

[1] N. Assrir, F. Malard, E. Lescop, *Results Probl Cell Differ* **2017**, *64*, 9-46.
[2] R. Amson, S. Pece, J. C. Marine, P. P. Di Fiore, A. Telerman, *Trends Cell Biol* **2013**, *23*, 37-46.
[3] T. Kawakami, T. Ando, Y. Kawakami, *The Open Allergy Journal* **2012**, *5*, 41-46.
[4] M. Nagano-Ito, S. Ichikawa, *Biochem. Res. Int.* **2012**, *2012*, 204960.
[5] T. H. Chan, L. Chen, X. Y. Guan, *Biochem Res Int* **2012**, *2012*, 369384.
[6] J. Acunzo, V. Baylot, A. So, P. Rocchi, *Cancer Treat. Rev.* **2014**, *40*, 760-9.
[7] A. Telerman, R. Amson, *Nat. Rev. Cancer* **2009**, *9*, 206-16.
[8] Y. Yang, F. Yang, Z. Xiong, Y. Yan, X. Wang, M. Nishino, D. Mirkovic, J. Nguyen, H. Wang, X. F. Yang, *Oncogene* **2005**, *24*, 4778-88.
[9] D. Zhang, F. Li, D. Weidner, Z. H. Mnjoyan, K. Fujise, *J. Biol. Chem.* **2002**, *277*, 37430-8.
[10] H. Liu, H. W. Peng, Y. S. Cheng, H. S. Yuan, H. F. Yang-Yen, *Mol. Cell. Biol.* **2005**, *25*, 3117-26.
[11] S. Thebault, M. Agez, X. Chi, J. Stojko, V. Cura, S. B. Telerman, L. Maillet, F. Gautier, I. Billas-Massobrio, C. Birck, N. Troffer-Charlier, T. Karafin, J. Honore, A. Senff-Ribeiro, S. Montessuit, C. M. Johnson, P. Juin, S. Cianferani, J. C. Martinou, D. W. Andrews, R. Amson, A. Telerman, J. Cavarelli, *Sci. Rep.* **2016**, *6*, 19725.
[12] D. Pinkaew, A. Chattopadhyay, M. D. King, P. Chunhacha, Z. Liu, H. L. Stevenson, Y. Chen, P. Sinthujaroen, O. M. McDougal, K. Fujise, *Nat. Commun.* **2017**, *8*, 18.
[13] J. H. Lee, S. B. Rho, S. Y. Park, T. Chun, *FEBS Lett* **2008**, *582*, 1210-8.
[14] P. Graidist, M. Yazawa, M. Tonganunt, A. Nakatomi, C. C. Lin, J. Y. Chang, A. Phongdara, K. Fujise, *Biochem. J.* **2007**, *408*, 181-91.
[15] S. B. Rho, J. H. Lee, M. S. Park, H. J. Byun, S. Kang, S. S. Seo, J. Y. Kim, S. Y. Park, *FEBS Lett.* **2011**, *585*, 29-35.
[16] Y. Chen, T. Fujita, D. Zhang, H. Doan, D. Pinkaew, Z. Liu, J. Wu, Y. Koide, A. Chiu, C. C. Lin, J. Y. Chang, K. H. Ruan, K. Fujise, *J. Biol. Chem.* **2011**, *286*, 32575-85.
[17] R. Amson, S. Pece, A. Lespagnol, R. Vyas, G. Mazzarol, D. Tosoni, I. Colaluca, G. Viale, S. Rodrigues-Ferreira, J. Wynendaele, O. Chaloin, J. Hoebeke, J. C. Marine, P. P. Di Fiore, A. Telerman, *Nat Med* **2012**, *18*, 91-9.
[18] V. Baylot, M. Katsogiannou, C. Andrieu, D. Taieb, J. Acunzo, S. Giusiano, L. Fazli, M. Gleave, C. Garrido, P. Rocchi, *Mol. Ther.* **2012**, *20*, 2244-56.
[19] G. Funston, W. Goh, S. J. Wei, Q. S. Tng, C. Brown, L. Jiah Tong, C. Verma, D. Lane, F. Ghadessy, *PLoS One* **2012**, *7*, e42642.
[20] F. Li, D. Zhang, K. Fujise, *J. Biol. Chem.* **2001**, *276*, 47542-9.
[21] P. Graidist, A. Phongdara, K. Fujise, *J. Biol. Chem.* **2004**, *279*, 40868-75.
[22] U. A. Bommer, K. L. Vine, P. Puri, M. Engel, L. Belfiore, K. Fildes, M. Batterham, A. Lochhead, M. Aghmesheh, *Cell. Commun. Signal.* **2017**, *15*, 9.
[23] S. Hangai, T. Kawamura, Y. Kimura, C. Y. Chang, S. Hibino, D. Yamamoto, Y. Nakai, R. Tateishi, M. Oshima, H. Oshima, T. Kodama, K. Moriya, K. Koike, H. Yanai, T. Taniguchi, *Nat Immunol* **2021**, *22*, 947-957.
[24] F. Malard, N. Assrir, M. Alami, S. Messaoudi, E. Lescop, T. Ha-Duong, *J Mol Biol* **2018**, *430*, 1621-1639.
[25] Y. Feng, D. Liu, H. Yao, J. Wang, *Arch Biochem Biophys* **2007**, *467*, 48-57.
[26] F. R. Yarm, *Mol Cell Biol* **2002**, *22*, 6209-21.
[27] S. D'Amico, E. K. Krasnowska, I. Manni, G. Toietta, S. Baldari, G. Piaggio, M. Ranalli, A. Gambacurta, C. Vernieri, F. Di Giacinto, F. Bernassola, F. de Braud, M. Lucibello, *Cells* **2020**, *9*.
[28] H. J. Jeon, S. Y. You, Y. S. Park, J. W. Chang, J. S. Kim, J. S. Oh, *Biochim Biophys Acta* **2016**, *1863*, 630-637.
[29] U. Cucchi, L. M. Gianellini, A. De Ponti, F. Sola, R. Alzani, V. Patton, A. Pezzoni, S. Troiani, M. B. Saccardo, S. Rizzi, M. L. Giorgini, P. Cappella, I. Beria, B. Valsasina, *Anticancer Res* **2010**, *30*, 4973-85.
[30] M. Lucibello, S. Adanti, E. Antelmi, D. Dezi, S. Ciafre, M. L. Carcangiu, M. Zonfrillo, G. Nicotera, L. Sica, F. De Braud, P. Pierimarchi, *Oncotarget* **2015**, *6*, 5275-91.
[31] D. Chapagai, G. Ramamoorthy, J. Varghese, E. Nurmemmedov, C. McInnes, M. D. Wyatt, *J Med Chem* **2021**, *64*, 9916-9925.
[32] T. M. Johnson, R. Antrobus, L. N. Johnson, *Biochemistry* **2008**, *47*, 3688-96.
[33] R. Amson, J. E. Karp, A. Telerman, *Curr Opin Oncol* **2013**, *25*, 59-65.
[34] R. Amson, C. Auclair, F. Andre, J. Karp, A. Telerman, *Results Probl Cell Differ* **2017**, *64*, 283-290.
[35] U. A. Bommer, A. Telerman, *Cells* **2020**, *9*
[36] W. L. Zhu, H. X. Cheng, N. Han, D. L. Liu, W. X. Zhu, B. L. Fan, F. L. Duan, *Anticancer Res* **2008**, *28*, 1575-80.
[37] M. Tuynder, G. Fiucci, S. Prieur, A. Lespagnol, A. Geant, S. Beaucourt, D. Duflaut, S. Besse, L. Susini, J. Cavarelli, D. Moras, R. Amson, A. Telerman, *Proc Natl Acad Sci U S A* **2004**, *101*, 15364-9.
[38] M. Tuynder, L. Susini, S. Prieur, S. Besse, G. Fiucci, R. Amson, A. Telerman, *Proc Natl Acad Sci U S A* **2002**, *99*, 14976-81.
[39] S. Karaki, S. Benizri, R. Mejias, V. Baylot, N. Branger, T. Nguyen, B. Vialet, K. Oumzil, P. Barthelemy, P. Rocchi, *J Control Release* **2017**, *258*, 1-9.
[40] N. Fischer, E. J. Seo, S. Abdelfatah, E. Fleischer, A. Klinger, T. Efferth, *Invest New Drugs* **2021**, *39*, 914-927.
[41] N. Fischer, E. J. Seo, A. Klinger, E. Fleischer, T. Efferth, *Chem Biol Interact* **2021**, *334*, 109349.
[42] O. Kadioglu, T. Efferth, *Invest New Drugs* **2016**, *34*, 515-521.
[43] E. J. Seo, T. Efferth, *Oncotarget* **2016**, *7*, 16818-39.
[44] G. Sicard, C. Paris, S. Giacometti, A. Rodallec, J. Ciccolini, P. Rocchi, R. Fanciullino, *Pharmaceutics* **2020**, *12*
[45] H. Wu, W. Gong, X. Yao, J. Wang, S. Perrett, Y. Feng, *J Biol Chem* **2015**, *290*, 8694-710.
[46] L. Bonnat, M. Dautriche, T. Saidi, J. Revol-Cavalier, J. Dejeu, E. Defrancq, T. Lavergne, *Org Biomol Chem* **2019**, *17*, 8726-8736.
[47] E. Laigre, D. Goyard, C. Tiertant, J. Dejeu, O. Renaudet, *Org Biomol Chem* **2018**, *16*, 8899-8903.
[48] B. Nguyen, F. A. Tanious, W. D. Wilson, *Methods* **2007**, *42*, 150-61.
[49] J. E. Gestwicki, H. V. Hsieh, J. B. Pitner, *Anal Chem* **2001**, *73*, 5732-7.
[50] D. Dell'Orco, K. W. Koch, *ACS Chem Biol* **2016**, *11*, 2390-7.
[51] D. Dell'Orco, S. Sulmann, S. Linse, K. W. Koch, *Anal Chem* **2012**, *84*, 2982-9.
[52] S. Sulmann, D. Dell'Orco, V. Marino, P. Behnen, K. W. Koch, *Chemistry* **2014**, *20*, 6756-62.
[53] H. MacDonald, H. Bonnet, A. Van der Heyden, E. Defrancq, N. Spinelli, L. Coche-Guérente, J. Dejeu, *J. Phys. Chem. C* **2019**, *123*, 13561-13568.
[54] F. H. Niesen, H. Berglund, M. Vedadi, *Nat Protoc* **2007**, *2*, 2212-21.
[55] V. Receveur-Brechot, D. Durand, *Curr Protein Pept Sci* **2012**, *13*, 55-75.
[56] Y. Liu, V. C. Chen, M. Lu, M. Lee, R. S. McIntyre, A. Majeed, Y. Lee, Y. Chen, *Cancers* **2020**, *12*, 1184.
[57] H. Chan, W. Chiu, V. C. Chen, K. Huang, T. Wang, Y. Lee, R. S. McIntyre, T. Hsu, C. T. Lee, B. Tzang, *Psycho-oncology* **2018**, *27*, 187-192.

[58] L. S. Morch, C. Dehlendorff, L. Baandrup, S. Friis, S. K. Kj\aer, *International journal of cancer* **2017**, *141*, 2197-2203.
[59] W. Xu, H. Tamim, S. Shapiro, M. R. Stang, J. Collet, *The lancet oncology* **2006**, *7*, 301-308.
[60] A. Zingone, D. Brown, E. D. Bowman, O. M. Vidal, J. Sage, J. Neal, B. M. Ryan, *Cancer treatment and research communications* **2017**, *10*, 33-39.
[61] G. Shoval, R. D. Balicer, B. Feldman, M. Hoshen, G. Eger, A. Weizman, G. Zalsman, B. Stubbs, P. Golubchik, B. Gordon, A. Krivoy, *Depression and anxiety* **2019**, *36*, 921-929.
[62] C. J. Lin, F. Robert, R. Sukarieh, S. Michnick, J. Pelletier, *Cancer Res* **2010**, *70*, 3199-208.
[63] X. Jiang, W. Lu, X. Shen, Q. Wang, J. Lv, M. Liu, F. Cheng, Z. Zhao, X. Pang, *JCI Insight* **2018**, *3*
[64] K. K. Reddy, B. Lefkove, L. B. Chen, B. Govindarajan, A. Carracedo, G. Velasco, C. O. Carrillo, S. S. Bhandarkar, M. J. Owens, F. Mechta-Grigoriou, J. Arbiser, *Pigment cell & melanoma research* **2008**, *21*, 451-456.
[65] J. Kuwahara, T. Yamada, N. Egashira, M. Ueda, N. Zukeyama, S. Ushio, S. Masuda, *Biological and Pharmaceutical Bulletin* **2015**, *38*, 1410-1414.
[66] D. Xia, Y. Zhang, G. Xu, W. Yan, X. Pan, J. Tong, *Leukemia & lymphoma* **2017**, *58*, 2208-2217.
[67] M. E. Di Rosso, H. A. Sterle, G. A. Cremaschi, A. M. Genaro, *Frontiers in immunology* **2018**, *9*, 1341.
[68] K. M. A. Zinnah, J. Seol, S. Park, *International Journal of Molecular Medicine* **2020**, *46*, 795-805.
[69] S. L. Geeraerts, K. R. Kampen, G. Rinaldi, P. Gupta, M. Planque, N. Louros, E. Heylen, K. De Cremer, K. De Brucker, S. Vereecke, B. Verbelen, P. Vermeersch, J. Schymkowitz, F. Rousseau, D. Cassiman, S. Fendt, A. Voet, B. P. A. Cammue, K. Thevissen, K. De Keersmaecker, *Molecular Cancer Therapeutics* **2021**, *20*, 50-63.
[70] S. Kang, S. M. Dong, B. R. Kim, M. S. Park, B. Trink, H. J. Byun, S. B. Rho, *Apoptosis* **2012**, *17*, 989-97.
[71] H. Yue, D. Huang, L. Qin, Z. Zheng, L. Hua, G. Wang, J. Huang, H. Huang, *BioMed research international* **2016**, *2016*
[72] T. Yin, S. He, G. Shen, T. Ye, F. Guo, Y. Wang, *Molecular medicine reports* **2015**, *12*, 4103-4108.
[73] C. Zhang, P. Gong, P. Liu, N. Zhou, Y. Zhou, Y. Wang, *Oncology reports* **2017**, *37*, 1168-1174.
[74] J. Mu, H. Xu, Y. Yang, W. Huang, J. Xiao, M. Li, Z. Tan, Q. Ding, L. Zhang, J. Lu, X. Wu, Y. Liu, *Oncology reports* **2014**, *31*, 2107-2114.
[75] M. Mao, T. Yu, J. Hu, L. Hu, *J Obstet Gynaecol Res* **2015**, *41*, 1240-5.
[76] S. Koch, S. K. Hemrick-Luecke, L. K. Thompson, D. C. Evans, P. G. Threlkeld, D. L. Nelson, K. W. Perry, F. P. Bymaster, *Neuropharmacology* **2003**, *45*, 935-944.
[77] P. Seeman, T. Tallerico, *Molecular psychiatry* **1998**, *3*, 123-134.
[78] P. Seeman, R. Corbett, H. H. Van Tol, *Neuropsychopharmacology* **1997**, *16*, 93-110.
[79] E. Richelson, *Mayo Clin Proc* **1994**, *69*, 1069-81.
[80] B. L. Roth, W. K. Kroeze, S. Patel, E. Lopez, *The Neuroscientist* **2000**, *6*, 252-262.
[81] X. Wang, Z. B. Wang, C. Luo, X. Y. Mao, X. Li, J. Y. Yin, W. Zhang, H. H. Zhou, Z. Q. Liu, *J Cancer* **2019**, *10*, 1622-1632.
[82] C. L. B. Kline, M. D. Ralff, A. R. Lulla, J. M. Wagner, P. H. Abbosh, D. T. Dicker, J. E. Allen, W. S. El-Deiry, *Neoplasia* **2018**, *20*, 80-91.
[83] M. Tegowski, C. Fan, A. S. Baldwin, *Journal of Biological Chemistry* **2018**, *293*, 15977-15990.
[84] M. Yong, T. Yu, S. Tian, S. Liu, J. Xu, J. Hu, L. Hu, *Oncol Lett* **2017**, *14*, 8171-8177.
[85] R. A. Saxton, D. M. Sabatini, *Cell* **2017**, *168*, 960-976.
[86] S. B. Rho, B. R. Kim, S. Kang, *Gynecol Oncol* **2011**, *120*, 121-7.
[87] H. J. Byun, J. H. Lee, B. R. Kim, S. Kang, S. M. Dong, M. S. Park, S. H. Lee, S. H. Park, S. B. Rho, *Microvasc Res* **2012**, *84*, 227-34.
[88] M. S. Park, S. M. Dong, B. Kim, S. H. Seo, S. Kang, E. Lee, S. Lee, S. B. Rho, *Oncotarget* **2014**, *5*, 4929.
[89] U. A. Bommer, V. Iadevaia, J. Chen, B. Knoch, M. Engel, C. G. Proud, *Cell Signal* **2015**, *27*, 1557-68.
[90] C. A. Goodman, A. M. Coenen, J. W. Frey, J. S. You, R. G. Barker, B. P. Frankish, R. M. Murphy, T. A. Hornberger, *Oncotarget* **2017**, *8*, 18754-18772.
[91] D. Kobayashi, M. Hirayama, Y. Komohara, S. Mizuguchi, M. Wilson Morifuji, H. Ihn, M. Takeya, A. Kuramochi, N. Araki, *J Biol Chem* **2014**, *289*, 26314-26.
[92] C. Gouveia Roque, C. E. Holt, *Front Mol Neurosci* **2018**, *11*, 399.
[93] G. Thomas, G. Thomas, H. Luther, *Proc Natl Acad Sci U S A* **1981**, *78*, 5712-6.
[94] P. Schanda, E. Kupce, B. Brutscher, *J Biomol NMR* **2005**, *33*, 199-211.
[95] A. Favier, B. Brutscher, *J Biomol NMR* **2011**, *49*, 9-15.
[96] E. Lescop, T. Kern, B. Brutscher, *J. Magn. Reson.* **2010**, *203*, 190-8.
[97] A. Favier, B. Brutscher, *J Biomol NMR* **2019**, *73*, 199-211.
[98] W. F. Vranken, W. Boucher, T. J. Stevens, R. H. Fogh, A. Pajon, M. Llinas, E. L. Ulrich, J. L. Markley, J. Ionides, E. D. Laue, *Proteins* **2005**, *59*, 687-96.
[99] F. Delaglio, S. Grzesiek, G. W. Vuister, G. Zhu, J. Pfeifer, A. Bax, *J. Biomol. NMR* **1995**, *6*, 277-293.
[100] P. Dosset, J. C. Hus, M. Blackledge, D. Marion, *J. Biomol. NMR* **2000**, *16*, 23-8.
[101] O. Frances, F. Fatemi, D. Pompon, E. Guittet, C. Sizun, J. Perez, E. Lescop, G. Truan, *Biophys. J.* **2015**, *108*, 1527-36.
[102] S. Dutka-Malen, P. Mazodier, B. Badet, *Biochimie* **1988**, *70*, 287-90.
[103] R. L. Rich, D. G. Myszka, *Curr Opin Biotechnol* **2000**, *11*, 54-61.
[104] G. David, J. P\'erez, *J. Appl. Cryst.* **2009**, *42*, 892-900.
[105] J. Perez, Y. Nishino, *Curr Opin Struct Biol* **2012**, *22*, 670-8.
[106] E. Brookes, P. Vachette, M. Rocco, J. Perez, *J Appl Crystallogr* **2016**, *49*, 1827-1841.
[107] R. P. Rambo, J. A. Tainer, *Nature* **2013**, *496*, 477-81.
[108] D. Franke, M. V. Petoukhov, P. V. Konarev, A. Panjkovich, A. Tuukkanen, H. D. T. Mertens, A. G. Kikhney, N. R. Hajizadeh, J. M. Franklin, C. M. Jeffries, D. I. Svergun, *J Appl Crystallogr* **2017**, *50*, 1212-1225.